

1 **A total energy error analysis of dynamical cores and**
2 **physics-dynamics coupling in the Community Atmosphere**
3 **Model (CAM)**

4 **Peter H. Lauritzen^{1*}, and David L. Williamson¹**

5 ¹National Center for Atmospheric Research, Boulder, Colorado, USA

6 **Key Points:**

- 7 • Spurious total energy dissipation in dynamical core is $-0.3W/m^2$ to $-1W/m^2$ at 1
8 degree
9 • Constant-pressure assumption in physics leads to $0.3W/m^2$ spurious total energy
10 source
11 • There can easily be compensating errors in total energy budget

*1850 Table Mesa Drive, Boulder, Colorado, USA

Corresponding author: Peter Hjort Lauritzen, pel@ucar.edu

12 **Abstract**

13 A closed total energy (TE) budget is of utmost importance in coupled climate system
 14 modeling; in particular, the dynamical core or physics-dynamics coupling should ideally
 15 not lead to spurious TE sources/sinks. To assess this in a global climate model, a detailed
 16 analysis of the spurious sources/sinks of TE in NCAR's Community Atmosphere Model
 17 (CAM) is given. This includes spurious sources/sinks associated with the parameteriza-
 18 tion suite, the dynamical core, TE definition discrepancies and physics-dynamics coupling.
 19 The latter leads to a detailed discussion of the pros and cons of various physics-dynamics
 20 coupling methods commonly used in climate/weather modeling.

21 **1 Introduction**

22 In coupled climate modeling with prognostic atmosphere, ocean, land, land-ice, and
 23 sea-ice components, it is important to conserve total energy (TE) to a high degree in each
 24 component individually and in the complete model to avoid spurious long term trends in
 25 the simulated Earth system. Conservation of TE in this context refers to having a closed
 26 TE budget. For example, the TE change in a column in the atmosphere is exactly balanced
 27 by the net sources/sinks given by the fluxes through the column. The fluxes into the at-
 28 mospheric component from the surface models must be balanced by the fluxes in the re-
 29 spective surface components and so on. Henceforth we will focus only on the atmospheric
 30 component which, in a numerical model, is split into a resolved-scale component (the dy-
 31 namical core) and a sub-grid-scale component (parameterizations or, in modeling jargon,
 32 physics). While there have been many studies on energy flow in the Earth system through
 33 analysis of re-analysis data and observations [Trenberth and Fasullo, 2018, and references
 34 herein], there has been less focus on spurious TE sources/sinks in numerical models.

35 The atmospheric equations of motion conserve TE but the discretizations used in cli-
 36 mate and weather models are usually not inherently TE conservative. Exact conservation
 37 is probably not necessary but conservation to within $\sim 0.01 \text{ W/m}^2$ has been considered
 38 sufficient to avoid spurious trends in century long simulations [Boville, 2000; Williamson
 39 *et al.*, 2015]. Spurious sources and sinks of TE can be introduced by the dynamical core,
 40 physics, physics-dynamics coupling as well as discrepancies between the TE of the con-
 41 tinuous and discrete equations of motion and for the physics. Hence the study of TE con-
 42 servation in comprehensive models of the atmosphere quickly becomes a quite complex
 43 and detailed matter. In addition there can easily be compensating errors in the system as a
 44 whole.

45 Here we focus on versions of the Community Atmosphere Model (CAM) that use
 46 the spectral-element [SE, Lauritzen *et al.*, 2018] and finite-volume [FV, Lin, 2004] dy-
 47 namical cores. These dynamical cores couple with physics in a time-split manner, i.e.
 48 physics receives a state updated by dynamics [see Williamson, 2002, for a discussion
 49 of time-split versus process split physics-dynamics coupling in the context of CAM]. In
 50 its pure time-split form the physics tendencies are added to the state previously produced
 51 by the dynamical core and the resulting state provides the initial state for the subsequent
 52 dynamical core calculation. We refer to this as *state-updating* (`ftype=1` in CAM code).
 53 Alternatively, when the dynamical core adopts a shorter time step than the physics, say
 54 `nsplit` sub-steps, then $(1/\text{nsplit})$ th of the physics-calculated tendency is added to the
 55 state before each dynamics sub-step. We refer to this modification of time-splitting as
 56 *dribbling* (`ftype=0`). CAM-FV uses the *state-update* (`ftype=1`) approach while CAM-SE
 57 has options to use *state-update* (`ftype=1`), *dribbling* (`ftype=0`) or a combination of the
 58 two i.e. mass-variables use *state-updating* and remaining variables use *dribbling*. We refer
 59 to this as *combination* (`ftype=2`). The *dribbling* variants can lead to spurious sources or
 60 sinks of TE (and mass) referred to here as physics-dynamics coupling errors.

61 The dynamical core usually has inherent or specified filters to control spurious noise
 62 near the grid scale which will lead to energy dissipation [Thuburn, 2008; Jablonowski

and Williamson, 2011]. Similarly models often have sponge layers to control the solution near the top of the model that may be a sink of TE. There are examples of numerical discretizations of the adiabatic frictionless equations motion that are designed so that TE is conserved in the absence of time-truncation and filtering errors [e.g., Eldred and Randall, 2017; McRae and Cotter, 2013], e.g., mimetic spectral-element discretizations such as the one used in the horizontal in CAM-SE [Taylor, 2011]. These provide consistency between the discrete momentum and thermodynamic equations leading to global conservation associated with the conversion of potential to kinetic energy. In spectral transform models it is customary to add the energy change due to explicit diffusion on momentum back as heating (referred to as frictional heating), so that the diffusion of momentum does not affect the TE budget [see, e.g., p.71 in Neale et al., 2012]. This is also done in CAM-SE [Lauritzen et al., 2018].

The purpose of this paper is to provide a detailed global TE analysis of CAM. We assess TE errors due to various steps in the model algorithms. The paper is outlined as follows. In section 2 the continuous TE formulas are given and a detailed description of spurious TE sources/sinks that can occur in a model as a whole, and the associated diagnostics used to perform the TE analysis, are defined. In section 3 the model is run in various configurations to assess their effects on TE conservation. This includes various physics-dynamics coupling experiments leading to a rather detailed discussion of mass budget closure. We also investigate the effect of using a limiter in the vertical remapping of momentum, assess energy discrepancy errors and impacts on TE of simplifying surface conditions and dry atmosphere experiments. The paper ends with conclusions.

2 Method

2.1 Defining total energy (TE)

In the following it is assumed that the model top and bottom are coordinate surfaces and that there is no flux of mass through the model top and bottom. In a dry hydrostatic atmosphere the TE equation integrated over the entire sphere is given by

$$\frac{d}{dt} \int_{z=z_s}^{z=z_{top}} \iint_S E_v \rho^{(d)} dA dz = \int_{z=z_s}^{z=z_{top}} \iint_S F_{net} \rho^{(d)} dA dz, \quad (1)$$

[e.g., Kasahara, 1974] where F_{net} is net flux calculated by the parameterizations (e.g., heating and momentum forcing), d/dt the total/material derivative, z_s is the height of the surface, S the sphere, $\rho^{(d)}$ the density of dry air, E_v is the TE and dA is an infinitesimal area on the sphere. E_v can be split into kinetic energy $K = \frac{1}{2}\mathbf{v}^2$ (\mathbf{v} is the wind vector), internal energy $c_v^{(d)}T$, where $c_v^{(d)}$ is the heat capacity of dry air at constant volume, and potential energy $\Phi = gz$

$$E_v = K + c_v^{(d)}T + \Phi. \quad (2)$$

If the vertical integral is performed in a mass-based vertical coordinate, e.g., pressure, then the integrated TE equation for a dry atmosphere can be written as

$$\frac{d}{dt} \int_{p=p_s}^{p=p_{top}} \iint_S E_p \rho^{(d)} dA dp + \frac{d}{dt} \iint_S \Phi_s p_s dA = \int_{p=p_s}^{p=p_{top}} \iint_S F_{net} \rho dA dp, \quad (3)$$

[e.g., Kasahara, 1974] where

$$E_p = K + c_p^{(d)}T. \quad (4)$$

In a moist atmosphere, however, there are several definitions of TE used in the literature related to what heat capacity is used for water vapor and whether or not condensates are accounted for in the energy equation. To explain the details of that we focus on the energy equation for CAM-SE.

CAM-SE is formulated using a terrain-following hybrid-sigma vertical coordinate η but the coordinate levels are defined in terms of dry air mass per unit area ($M^{(d)}$) instead of total air mass; $\eta^{(d)}$ [see Lauritzen et al., 2018, for details]. In such a coordinate

106 system it is convenient to define the tracer state in terms of a dry mixing ratio instead of
 107 moist mixing ratio

$$m^{(\ell)} \equiv \frac{\rho^{(\ell)}}{\rho^{(d)}}, \text{ where } \ell = 'wv', 'cl', 'ci', 'rn', 'sw', \quad (5)$$

108 where $\rho^{(d)}$ is the mass of dry air per unit volume of moist air and $\rho^{(\ell)}$ is the mass of the
 109 water substance of type ℓ per unit volume of moist air. Moist air refers to air containing
 110 dry air ('d'), water vapor ('wv'), cloud liquid ('cl'), cloud ice ('ci'), rain amount ('rn')
 111 and snow amount ('sw'). For notational purposes define the set of all components of air

$$\mathcal{L}_{all} = \{'d', 'wv', 'cl', 'ci', 'rn', 'sw'\}, \quad (6)$$

112 Define associated heat capacities at constant pressure $c_p^{(\ell)}$. We refer to condensates as being
 113 *thermodynamically active* if they are included in the thermodynamic equation and mo-
 114 mentum equations. E.g. if the thermodynamic equation is formulated in terms of temper-
 115 ature the energy conversion term includes a generalized heat capacity which is a function
 116 of the condensates and their associated heat capacities [see, e.g., section 2.3 in *Lauritzen*
 117 *et al.*, 2018]. Similarly the weight of the condensates is included in the pressure field and
 118 pressure gradient force. How many and which condensates are thermodynamically ac-
 119 tive in the dynamical core is controlled with namelist `qsize_condensate_loading`. If
 120 `qsize_condensate_loading=1` only water vapor ('wv') is active, `qsize_condensate_loading=3`
 121 'wv', 'cl', and 'ci' are active, and if `qsize_condensate_loading=5` then 'wv', 'cl', 'ci', 'rn',
 122 and 'sw' are included.

123 Using the $\eta^{(d)}$ vertical coordinate and dry mixing ratios the TE (per unit area) that
 124 the frictionless adiabatic equations of motion in the CAM-SE dynamical core conserves is

$$\widehat{E}_{dyn} = \frac{1}{\Delta S} \int_{\eta=0}^{\eta=1} \iint_S \left(\frac{1}{g} \frac{\partial M^{(d)}}{\partial \eta^{(d)}} \right) \sum_{\ell \in \mathcal{L}_{all}} \left[m^{(\ell)} (K + c_p^{(\ell)} T + \Phi_s) \right] dA d\eta^{(d)}, \quad (7)$$

125 where ΔS is the surface area of the sphere, Φ_s is the surface geopotential and (\cdot) refers to
 126 the global average.

127 In the CAM physical parameterizations a different definition of TE is used. Due to
 128 the evolutionary nature of the model development, the parameterizations have not yet been
 129 converted to match the SE dynamical core. For the computation of TE, condensates are
 130 assumed to be zero and the heat capacity of moisture is the same as for dry air. This is
 131 equivalent to using a moist mass (dry air plus water vapor) but c_p of dry air:

$$\widehat{E}_{phys} = \frac{1}{\Delta S} \int_{\eta=0}^{\eta=1} \iint_S \left(\frac{1}{g} \frac{\partial M^{(d)}}{\partial \eta^{(d)}} \right) (1 + m^{(wv)}) \left[(K + c_p^{(d)} T + \Phi_s) \right] dA d\eta^{(d)}. \quad (8)$$

132 We note that earlier versions of CAM using the spectral transform dynamical core used
 133 c_p of moist air. The adiabatic, frictionless equations of motion in the CAM-SE dynamical
 134 core can be made consistent with E_{phys} by not including condensates in the mass/pressure
 135 field as well as energy conversion term in the thermodynamic equation and setting the
 136 heat capacity for moisture to $c_p^{(d)}$ [Taylor, 2011]. We refer to this version of CAM-SE as
 137 the *energy consistent* version.

138 2.2 Spurious energy sources and sinks

139 In a weather/climate model TE conservation errors can appear in many places through-
 140 out the algorithm. Below is a general list of where conservation errors can appear with
 141 specific examples from CAM:

- 142 1. *Parameterization errors*: Individual parameterizations may not have a closed en-
 143 ergy budget. CAM parameterizations are required to have a closed energy budget
 144 under the assumption that pressure remains constant during the computation of the

- 145 subgrid-scale parameterization tendencies. In other words, the TE change in the
 146 column is exactly balanced by the net sources/sinks given by the fluxes through the
 147 column.
- 148 2. *Pressure work error*: That said, if parameterizations update specific humidity then
 149 the surface pressure changes (e.g., moisture entering or leaving the column). In
 150 that case the pressure changes which, in turn, changes TE. This is referred to as
 151 *pressure work error* [section 3.1.8 in *Neale et al.*, 2012].
- 152 3. *Continuous TE formula discrepancy*: If the continuous equations of motion for the
 153 dynamical core conserve a TE different from the one used in the parameterizations
 154 then an energy inconsistency is present in the system as a whole. This is the case
 155 with the new version of CAM-SE that conserves a TE that is more accurate and
 156 comprehensive than that used in the CAM physics package as discussed above. As
 157 also noted above, this mismatch arose from the evolutionary nature of the model
 158 development and not by deliberate design; and should be eliminated in the future.
- 159 4. *Dynamical core errors*: Energy conservation errors in the dynamical core, not re-
 160 lated to physics-dynamics coupling errors, can arise in multiple parts of the algo-
 161 rithms used to solve the equations of motion. For dynamical cores employing fil-
 162 tering [e.g., limiters in flux operators *Lin*, 2004] and/or possessing inherent damp-
 163 ing which controls small scales, it is hard to isolate their energy dissipation from
 164 other errors in the discretization. If a hyperviscosity term or some other diffusion
 165 is added to the momentum equation, then one can diagnose the local energy dissis-
 166 pation from such damping and add a corresponding heating to balance it (frictional
 167 heating). There may also be energy loss from viscosity applied to other variables
 168 such as temperature or pressure which is harder to compensate. Here is a break-down
 169 relevant to CAM-SE using a floating Lagrangian vertical coordinate:
- 170 • Horizontal inviscid dynamics: Energy errors resulting from solving the inviscid,
 171 adiabatic equations of motion.
 - 172 • Hyperviscosity: Filtering errors.
 - 173 • Vertical remapping: The vertical remapping algorithm from Lagrangian to Eule-
 174 rian reference surfaces does not conserve TE.
 - 175 • Near round-off negative values of water vapor which are filled to a minimal
 176 value without compensation.
- 177 5. *Physics-dynamics coupling (PDC)*: Assume that physics computes a tendency. Usu-
 178 ally the tendency (forcing) is passed to the dynamical core which is responsible for
 179 adding the tendencies to the state. PDC energy errors can be split into three types:
- 180 • ‘Dribbling’ errors (or, equivalently, temporal PDC errors): If the TE increment
 181 from the parameterizations does not match the change in TE when the tenden-
 182 cies are added to the state in the dynamical core, then there will be a spurious
 183 PDC error. This will not happen with the *state-update* approach in which the
 184 tendencies are added immediately after physics and before the dynamical core
 185 advances the solution in time.
 - 186 • Change of vertical grid/coordinate errors: If the vertical coordinates in physics
 187 and in the dynamical core are different then there can be spurious PDC energy
 188 errors even when using the state-update method for adding tendencies to the dy-
 189 namical core state. For example, many non-hydrostatic dynamical cores [e.g.
 190 *Skamarock et al.*, 2012] use a terrain-following height coordinate whereas physics
 191 uses pressure.
 - 192 • Change of horizontal grid errors: If the physics tendencies are computed on a
 193 different horizontal grid than the dynamical core then there can be spurious en-
 194 ergy errors from mapping tendencies and/or variables between horizontal grids
 195 [e.g., *Herrington et al.*, 2018].
- 196 6. *Compensating Energy fixers*: To avoid TE conservation errors which could accu-
 197 mulate and ultimately lead to a climate drift, it is customary to apply an arbitrary

198 energy fixer to restore TE conservation. Since the spatial distribution of many en-
 199 ergy errors, in general, is not known, global fixers are used. In CAM a uniform in-
 200 crement is added to the temperature field to compensate for TE imbalance from all
 201 processes, i.e. dynamical core, physics-dynamics coupling, TE formula discrepancy,
 202 energy change due to pressure work **error**, and possibly parameterization errors if
 203 present.

204 2.3 Diagnostics

205 The discrete global averages (\cdot) are computed consistent with the discrete model grid
 206 as outlined in section 2.2. of *Lauritzen et al. [2014]*. The TE global average tendency is
 207 denoted

$$\partial \widehat{E} \equiv \frac{d \widehat{E}}{dt}. \quad (9)$$

208 By computing the global TE averages \widehat{E} at appropriate places in the model algorithms,
 209 we can directly compute $\partial \widehat{E}$ due to various processes (such as viscosity, vertical remap-
 210 ping, physics-dynamics coupling, pressure work **error**, etc.) by differencing \widehat{E} from after
 211 and before the algorithm takes place. This has been implemented using CAM history in-
 212 frastructure by computing column integrals of energy at various places in CAM and out-
 213 putting the 2D energy fields. CAM history internally handles accumulation and averag-
 214 ing in time at each horizontal grid point. The global averages are computed externally
 215 from the grid point vertical integrals on the history files (stored in double precision). The
 216 places in CAM where we compute/capture the grid point vertical integral E are named us-
 217 ing three letters where the first letter refers to whether the vertical integral is performed
 218 in physics ('p') or in the dynamical core ('d'). The trailing two letters refer to the specific
 219 location in dynamics or physics. For example, 'BP' refers to 'Before Physics' and 'AP'
 220 to 'After Physics'; the associated total energies are denoted E_{pBP} and E_{pAP} , respectively.
 221 The TE tendency from the parameterizations is the difference between E_{pBP} and E_{pAP}
 222 divided by the time-step. The terms and tendencies are then averaged globally externally
 223 to the model. The pseudo-code in Figure 1 defines the acronyms in terms of where in the
 224 CAM-SE algorithm the TE vertical integrals are computed and output. For details on the
 225 CAM-SE algorithm please see *Lauritzen et al. [2018]*.

226 Before defining the individual terms in detail we briefly review the model time step-
 227 ping sequence starting with the physics component as illustrated in Figure 1. The energy
 228 fixer is applied first to compensate for the spurious net energy change from all compo-
 229 nents introduced during the previous time step. We will describe this in more detail af-
 230 ter the various sources and sinks are elucidated. The parameterizations are applied next
 231 and are required to be energy conserving. They update the state and accumulate the total
 232 physics tendency (forcing). At this stage the state is saved for use in the energy fixer in
 233 the next time step. Any changes in the global average energy after this are spurious and
 234 are compensated by the fixer. The parameterizations update the water vapor but not the
 235 moist pressure, implying a non-physical change in the dry mass of the atmosphere. The
 236 dry mass correction corrects the dry mass back to its proper value.

237 The forcing (physics tendency) from the parameterizations is passed to the dynam-
 238 ical core. If the physics and dynamics operate on different grids, the forcing is remapped
 239 here. The dynamics operates on a shorter time step the physics and is sub-stepped. The
 240 remapped forcing is applied to the dynamics state, saved from the end of the previous
 241 dynamics step, using either *state-updating*, *dribbling*, or *combination* as described in the
 242 introduction. The dynamics then advances the adiabatic frictionless flow in the floating
 243 Lagrangian layers over a further set of sub-steps. Hyperviscosity is applied next with fur-
 244 ther sub-stepping required for computational stability of the explicit discrete approxima-
 245 tions. The energy loss from the specified momentum viscosity is calculate locally and is
 246 balanced by adding a local change to the temperature, referred to as *frictional heating*.
 247 This set of dynamics sub-steps is followed by the vertical remapping from Lagrangian to

248 Eulerian reference layers. The remapping is required to provide layers consistent with the
 249 parameterization formulations. The vertical remapping sub-steps are required for stability
 250 if the Lagrangian layers become too thin.

251 At the end of the dynamics, the state is saved to be used by the dynamics the next
 252 time step and is also passed to the physics, with a remapping if the dynamics and physics
 253 grids differ. At the beginning of the physics the difference in energy between this state
 254 and the state saved after the physics during the previous time step is the amount needed to
 255 be added or subtracted by the energy fixer. It represents the accumulation of all spurious
 256 sources from the dry mass correction, remappings between physics and dynamics grids
 257 (if applicable), dynamical core, differing energy definitions (if present), hyerviscosity, and
 258 vertical remapping.

267 We now define the following energy tendencies corresponding to the itemized list in
 268 section 2.2 with references to terms indicated in Figure 1. We start just after the energy
 269 fixer which will be defined at the end.

- 270 1. $\partial\widehat{E}^{(param)}$: TE tendency due to parameterizations. In CAM the TE budget for each
 271 parameterization is closed (assuming pressure is unchanged) so $\partial\widehat{E}^{(param)}$ is bal-
 272 anced by net fluxes in/out of the physics columns. Note that this is the only energy
 273 tendency that is not spurious since CAM parameterizations have a closed TE bud-
 274 get. This TE tendency is discretely computed as

$$\partial\widehat{E}_{phys}^{(param)} = \frac{\widehat{E}_{pAP} - \widehat{E}_{pBP}}{\Delta t_{phys}}, \quad (10)$$

275 where Δt_{phys} is the physics time-step (default 1800s) and the subscript *phys* on $\partial\widehat{E}$
 276 refers to the energy tendency computed in CAM physics.

- 277 2. $\partial\widehat{E}^{(pwork)}$: Total spurious energy tendency due to pressure work **error**

$$\partial\widehat{E}_{phys}^{(pwork)} = \frac{\widehat{E}_{pAM} - \widehat{E}_{pAP}}{\Delta t_{phys}}. \quad (11)$$

278 Since CAM-SE dynamical core is based on a dry-mass vertical coordinate the pres-
 279 sure work **error** takes place implicitly in the dynamical core. But the TE tendency
 280 due to pressure work **error** is conveniently computed in physics since dynamical
 281 cores based on a moist vertical coordinate (e.g., CAM-FV) require pressure and
 282 moist mixing ratios to be adjusted for dry mass conservation and tracer mass con-
 283 servation [section 3.1.8 in *Neale et al.*, 2012]. The difference of TE after and be-
 284 fore this adjustment is the TE tendency due to pressure work **error**. In a dry mass
 285 vertical coordinate based on dry mixing ratios neither dry mass layer thickness nor
 286 dry mixing ratios need to be adjusted to take into account moisture changes in the
 287 column. For labeling purposes, the 'total forcing' associated with physics (at least
 288 in CAM) consists of parameterizations, pressure work **error** and TE fixer, although
 289 strictly speaking the fixer includes components from the dynamics as will be seen.

$$\partial\widehat{E}_{phys}^{(phys)} \equiv \partial\widehat{E}_{phys}^{(param)} + \partial\widehat{E}_{phys}^{(pwork)} + \partial\widehat{E}_{phys}^{(efix)} = \frac{\widehat{E}_{pAM} - \widehat{E}_{pBF}}{\Delta t_{phys}}. \quad (12)$$

290 where the energy fixer TE tendency is

$$\partial\widehat{E}_{phys}^{(efix)} = \frac{\widehat{E}_{pBP} - \widehat{E}_{pBF}}{\Delta t_{phys}}. \quad (13)$$

291 After all the TE budget terms have been defined, the exact composition of $\partial\widehat{E}_{phys}^{(efix)}$
 292 will be presented.

- 293 3. $\partial\widehat{E}^{(discr)}$: If the physics uses a TE definition different from the TE that the con-
 294 tinuous equations of motion in the dynamical core conserve (i.e. in the absence of

discretization errors), then there is a TE discrepancy tendency. This complicates the energy analysis as one can not compare TE computed in physics \widehat{E}_{phys} directly with TE computed in the dynamical core \widehat{E}_{dyn} . This makes errors associated with this discrepancy tricky to assess. That said, the TE tendencies computed using the dynamical core TE formula $\partial\widehat{E}_{dyn}$ are well defined (self consistent) and similarly for TE tendencies computed using the ‘physics formula’ for TE, $\partial\widehat{E}_{phys}$.

4. The TE tendency from the dynamical core is split into several terms: Horizontal adiabatic dynamics (dynamics excluding physics forcing tendency)

$$\partial\widehat{E}_{dyn}^{(2D)} = \frac{\widehat{E}_{dAD} - \widehat{E}_{dBH}}{\Delta t_{dyn}}, \quad (14)$$

where over a single dynamics sub-step $\Delta t_{dyn} = \frac{\Delta t_{phys}}{n_{split} \times r_{split}}$ (the loop bounds n_{split} , r_{split} , etc. are explained in Figure 1).

In CAM-SE the viscosity is explicit so one can compute the TE tendency due to hyperviscosity and its associated frictional heating

$$\partial\widehat{E}_{dyn}^{(hvis)} = \frac{\widehat{E}_{dAH} - \widehat{E}_{dBH}}{\Delta t_{hvis}}, \quad (15)$$

which, in CAM-SE, includes a frictional heating term from viscosity on momentum

$$\partial\widehat{E}_{dyn}^{(fheat)} = \frac{\widehat{E}_{dAH} - \widehat{E}_{dCH}}{\Delta t_{hvis}}, \quad (16)$$

where $\Delta t_{hvis} = \frac{\Delta t_{phys}}{n_{split} \times r_{split} \times h_{viscous_subcycle}}$ is the time step of the sub-stepped viscosity. The residual

$$\partial\widehat{E}_{dyn}^{(res)} = \partial\widehat{E}_{dyn}^{(2D)} - \partial\widehat{E}_{dyn}^{(hvis)}, \quad (17)$$

is the energy error due to inviscid dynamics and time-truncation errors.

The energy tendency due to vertical remapping is

$$\partial\widehat{E}_{dyn}^{(remap)} = \frac{\widehat{E}_{dAR} - \widehat{E}_{dAD}}{\Delta t_{remap}}, \quad (18)$$

where $\Delta t_{remap} = \frac{\Delta t_{phys}}{n_{split}}$.

The 3D adiabatic dynamical core (no physics forcing but including friction) energy tendency is denoted

$$\partial\widehat{E}_{dyn}^{(adiab)} = \partial\widehat{E}_{dyn}^{(2D)} + \partial\widehat{E}_{dyn}^{(remap)}. \quad (19)$$

5. $\partial\widehat{E}^{(pdc)}$: Total spurious energy tendency due to physics-dynamics coupling errors is the difference between the energy tendency from physics and the energy tendency in the dynamics resulting from adding the physics increment to the dynamical core state

$$\partial\widehat{E}^{(pdc)} = \partial\widehat{E}_{phys}^{(phys)} - \partial\widehat{E}_{dyn}^{(phys)} \text{ assuming } \partial\widehat{E}^{(discr)} = 0, \quad (20)$$

where

$$\partial\widehat{E}_{dyn}^{(phys)} = \frac{\widehat{E}_{dBD} - \widehat{E}_{dAF}}{\Delta t_{pdc}}, \quad (21)$$

and Δt_{pdc} is the time-step between physics increments being added to the dynamical core. Remember we are dealing with average rates so terms computed with different time steps can be compared, but differences cannot be taken between terms sampled with different time steps.

The physics-dynamics coupling TE tendency $\partial\widehat{E}^{(pdc)}$ makes use of TE formulas in dynamics and in physics so (20) is only well-defined if the TE formula discrepancy is zero, $\partial\widehat{E}^{(discr)} = 0$. As mentioned in Section 2.1, CAM-SE has the option to switch the continuous equations of motion conserving the TE used by CAM physics (8) instead of the more comprehensive TE formula (7).

In CAM-SE there are 3 physics-dynamics coupling algorithms described in detail in section 3.6 in *Lauritzen et al.* [2018] and reviewed in the introduction here. One is *state-update* in which the entire physics increments are added to the dynamics state at the beginning of dynamics (referred to as `ftype=1`), in which case $\Delta t_{pdc} = \Delta t_{phys}$. Another is *dribbling* in which the physics tendency is split into `nsplit` equal chunks and added throughout dynamics (more precisely after every vertical remapping; referred to as `ftype=0` resulting in $\Delta t_{pdc} = \frac{1}{n\text{split}}\Delta t_{phys}$), and then a *combination* of the two (referred to as `ftype=2`) where tracers (mass variables) use *state-update* (`ftype=1`) and all other physics tendencies use *dribbling* (`ftype=0`).

6. $\partial\widehat{E}^{(efix)}$: Global energy fixer tendency, defined in (13), is applied at the beginning of the parameterizations. The correction needed is the global average difference between the state passed from the dynamics and the state that was saved after the physics updated the state but before the dry mass correction. It includes all spurious sources from the dry mass correction, remappings between physics and dynamics, dynamical core, differing energy definitions (if present), hyperviscosity, and vertical remapping.

2.4 A few observations regarding the energy budget terms

It is useful to note that the energy fixer ‘fixes’ energy errors for the dynamical core, pressure work **error**, physics-dynamics coupling and TE discrepancy

$$-\partial\widehat{E}_{phys}^{(efix)} = \partial\widehat{E}_{phys}^{(pwork)} + \partial\widehat{E}_{dyn}^{(adiab)} + \partial\widehat{E}^{(pdc)} + \partial\widehat{E}^{(discr)}. \quad (22)$$

The forcing from the parameterizations, $\partial\widehat{E}_{phys}^{(param)}$, does not appear in this budget (although the dynamical core state does ‘feel’ the parameterization forcing) as the energy cycle for the parameterizations is, by design in CAM, closed (balanced by fluxes in/out of the physics columns). If $\partial\widehat{E}^{(discr)} = 0$, one can use (22) to diagnose energy dissipation in the dynamical core and physics-dynamics coupling from quantities computed only in physics

$$\partial\widehat{E}_{dyn}^{(adiab)} + \partial\widehat{E}^{(pdc)} = -\partial\widehat{E}_{phys}^{(efix)} - \partial\widehat{E}_{phys}^{(pwork)} \text{ for } \partial\widehat{E}^{(discr)} = 0. \quad (23)$$

This is useful if the diagnostics are not implemented in the dynamical core; in particular, if the *state-update* (`ftype=1`) physics-dynamics coupling method is used then $\partial\widehat{E}^{(pdc)} = 0$ and the TE errors in the dynamical core can be computed without diagnostics implemented in the dynamical core. Also, (23) provides an alternative formula for $\partial\widehat{E}^{(pdc)}$ compared to (20):

$$\partial\widehat{E}^{(pdc)} = -\partial\widehat{E}_{phys}^{(efix)} - \partial\widehat{E}_{phys}^{(pwork)} - \partial\widehat{E}_{dyn}^{(adiab)} \text{ assuming } \partial\widehat{E}^{(discr)} = 0. \quad (24)$$

If $\partial\widehat{E}^{(pdc)} = 0$ (22) can be used to compute $\partial\widehat{E}^{(discr)}$

$$\partial\widehat{E}^{(discr)} = -\partial\widehat{E}_{phys}^{(efix)} - \partial\widehat{E}_{phys}^{(pwork)} - \partial\widehat{E}_{dyn}^{(adiab)}, \text{ assuming } \partial\widehat{E}^{(pdc)} = 0. \quad (25)$$

Note that we can not use (20) to compute $\partial\widehat{E}^{(discr)}$ since $\widehat{E}_{phys} \neq \widehat{E}_{dyn}$.

3 Results

A series of simulations have been performed with CESM2.1 using CAM version 6 (CAM6) physics (<https://doi.org/10.5065/D67H1H0V>) on NCAR’s Cheyenne cluster [*Computational and Information Systems Laboratory*, 2017]. All simulations are at nominally $\sim 1^\circ$ horizontal resolution (for CAM-SE that is 30×30 elements on each cubed-sphere face and for CAM-FV its 192×288 latitudes-longitudes) and using the standard 32 levels in the vertical. Unless otherwise noted all simulations are 13 months in duration and the last 12 months are used in the analysis. Total energy budgets are summarized in Table 1 and discussed below. The first column gives identifying ‘Descriptors’ which

Table 1. TE tendencies in units of W/m^2 associated with various aspects of CAM-SE run in AMIP-type setup (unless otherwise noted). Column 1 is the identifier for the model configuration. See the text for a brief summary of these descriptors. They are defined in more detail in the following sections where the section titles also include the ‘Descriptor’ from Table 1 to make it easier for the reader to match Table entries with discussion in the text. Column 2 is \mathcal{N} =qsize_condensate_loading identifying how many water species are thermodynamically active in the dynamical core (see section 2.1 for details). Column 3, lcp_moist, indicates whether or not the heat capacity includes water variables or not and column 4 shows physics-dynamics coupling method ftype. The TE tendencies $\partial \widehat{E}$ in columns 5-14 are defined in section 2.3. If $\partial \widehat{E}$ is less than $10^{-5} W/m^2$ it is set to zero in the Table. Significant changes compared to the baseline (TE consistent configuration) discussed in the main text are in bold font.

Descriptor	\mathcal{N}	lcp_moist	ftype	$\partial \widehat{E}_{phys}^{(pwork)}$	$\partial \widehat{E}_{phys}^{(efix)}$	$\partial \widehat{E}_{phys}^{(discr)}$	$\partial \widehat{E}_{dyn}^{(2D)}$	$\partial \widehat{E}_{dyn}^{(heat)}$	$\partial \widehat{E}_{dyn}^{(vis)}$	$\partial \widehat{E}_{dyn}^{(res)}$	$\partial \widehat{E}_{dyn}^{(fmap)}$	$\partial \widehat{E}_{dyn}^{(adiab)}$	$\partial \widehat{E}_{dyn}^{(remap)}$	$\partial \widehat{E}_{dyn}^{(dyn)}$	$\partial \widehat{E}^{(pd)}$
<i>TE consistent</i>	1	false	1	0.312	0.300	0	-0.601	-0.608	0.565	0.007	-0.011	-0.613	-0.613	0	
‘dribbling’ A	1	false	0	0.315	0.313	0	-0.577	-0.584	0.568	0.007	-0.011	-0.588	-0.588	0.469	
‘dribbling’ B	1	false	2	0.316	0.341	0	-0.598	-0.606	0.563	0.008	-0.011	-0.609	-0.609	0.484	
<i>vert limiter</i>	1	false	1	0.317	0.472	0	-0.590	-0.597	0.509	0.006	-0.199	-0.789	-0.789	0	
<i>smooth topo</i>	1	false	1	0.315	-0.008	0	-0.295	-0.300	0.493	0.005	-0.012	-0.307	-0.307	0	
<i>energy discr</i>	5	true	1	0.332	-0.313	0.594	-0.603	-0.612	0.575	0.009	-0.011	-0.614	-0.614	-	
<i>default</i>	5	true	2	0.316	-0.272	-0.578	-0.587	-0.579	0.579	0.010	-0.012	-0.589	-0.589	-	
<i>QPC6</i>	1	false	1	0.305	-0.169	0	-0.129	-0.131	0.477	0.001	-0.007	-0.136	-0.136	0	
<i>FHS94</i>	1	false	2	-	-	-0.025	-0.025	0.122	0	0.005	-0.020	-0.020	-	-	
<i>FV</i>	1	false	1	0.304	0.670	0	-	-	-	-	-	-0.974	-0.974	0	
<i>CSLAM</i>	1	false	1	0.312	0.239	0	-0.547	-0.557	0.620	0.010	-0.011	-0.558	-0.558	-0.070	
<i>CSLAM default</i>	5	true	2	0.320	-0.342	-	-0.524	-0.537	0.641	0.013	-0.011	-0.535	-0.535	-	

370 are briefly summarized below and defined in more detail in the following sections. The
 371 section titles also include the ‘Descriptor’ from Table 1 to make it easier for the reader
 372 to match Table entries with discussion in the text. Important changes to TE errors are
 373 marked with bold font in Table 1.

374 Various configurations are used and referred to in terms of the *COMPSET* (Com-
 375 ponent Set) value used in CESM2.1. The *COMPSET F2000climo* configuration refers
 376 to ‘real-world’ AMIP (Atmospheric Model Intercomparison Project) type simulations us-
 377 ing perpetual year 2000 SST (Sea Surface Temperature) boundary conditions. The first 7
 378 simulations in the table (those above the horizontal line) are such AMIP-type simulations
 379 (*F2000climo*) with the first serving as a control for the 6 following variants. The remain-
 380 ing 5 simulation descriptors (below the horizontal line in Table 1) list their *COMPSET* or
 381 dynamical core settings.

- 382 • *TE consistent*: The TE consistent version uses *state update* physics-dynamics cou-
 383 pling (*ftype* 1) described in section 3.1,
- 384 • ‘*dribbling*’ A: as *TE consistent* but with *dribbling* physics-dynamics coupling (*ftype*
 385 0) (section 3.2),
- 386 • ‘*dribbling*’ B: as *TE consistent* but with *dribbling* combination physics-dynamics
 387 coupling (*ftype* 2) (section 3.2),
- 388 • *vert limiter*: as *TE consistent* but using limiters in the vertical remapping of mo-
 389 mentum (section 3.3),
- 390 • *smooth topo*: as *TE consistent* but using smoother topography (see section 3.4),
- 391 • *energy discr*: The version with energy discrepancy (but no physics-dynamics cou-
 392 pling errors) described in section 3.5,
- 393 • *default*: as *energy discr* version but with *ftype*=2 which is the current default
 394 CAM-SE (section 3.5),
- 395 • *QPC6*: A simplified aqua-planet setup based on the *TE consistent*, i.e an aqua-
 396 planet setup using CAM6 physics; an ocean covered planet in perpetual equinox,
 397 with fixed, zonally symmetric sea surface temperatures [Neale and Hoskins, 2000;
 398 Medeiros et al., 2016] (section 3.6),
- 399 • *FSH94*: Dry dynamical core configuration based on Held-Suarez forcing which re-
 400 laxes temperature to a zonally symmetric equilibrium temperature profile and sim-
 401 ple linear drag at the lower boundary [Held and Suarez, 1994] (section 3.7).,
- 402 • *FV*: A configuration with the SE dynamical core replaced with the finite-volume
 403 core (section 3.8), and
- 404 • *CSLAM*: The quasi equal-area physics grid configuration of CAM-SE based on the
 405 TE consistent setup (section 3.9)
- 406 • *CSLAM default*: Same as *CSLAM* configuration but with *ftype*=2 and all forms of
 407 water thermodynamically active in the dynamical core.

414 3.1 *TE consistent: state-update physics-dynamics coupling (ftype=1) and no TE* 415 *formula discrepancy*

416 This configuration is the most energetically consistent in that the physical parame-
 417 terizations and the continuous equations of motion on which the dynamical core is based,
 418 conserve the same TE (defined in equation (8)); and there are no spurious sources/sinks in
 419 physics-dynamics coupling. Energetic consistency in dynamics and physics is obtained
 420 by setting $c_p^{(\ell)} \equiv c_p^d$ and $\mathcal{L}_{all} = \{‘d’, ‘wv’\}$ in the dynamical core equations of mo-
 421 tion and TE computations. Associated namelist changes resulting in this configuration are
 422 `lcp_moist = .false., se_qsize_condensate_loading = 1, and ftype = 1.`

423 The TE consistent configuration in AMIP-type simulation (*F2000climo*) is used to
 424 compute baseline TE tendencies which will be used to compare with other model con-
 425 figurations. First we establish how long an average is needed to get robust TE tendency

estimates. Figure 2 shows $\partial\hat{E}$ for various aspects of CAM-SE as a function of time. The simulation length is 5 years and monthly average values are used for the analysis. First consider the left plot. The TE tendency from parameterizations ($\partial\hat{E}_{phys}^{(param)}$) show significant variability with an amplitude of approximately $2.5W/m^2$. As noted above this term does not figure in the spurious TE budget. The net source/sink provides an equal and opposite term to balance it. That said, the variability is reflected onto the TE tendency due to pressure work **error** $\partial\hat{E}_{phys}^{(pwork)} \approx 0.32 \pm 0.08W/m^2$. On the scale used in the left-hand plot the TE tendency of the adiabatic dynamical core $\partial\hat{E}_{dyn}^{(adiab)}$ does not seem to be affected by $\partial\hat{E}_{phys}^{(param)}$ or $\partial\hat{E}_{phys}^{(pwork)}$ in terms of variability, and remains stable at approximately $-0.6W/m^2 \pm 0.02W/m^2$. The TE fixer, in this model configuration, fixes $\partial\hat{E}_{dyn}^{(adiab)}$ and $\partial\hat{E}_{phys}^{(pwork)}$. Since the TE imbalance in the adiabatic dynamics remains approximately constant and the TE tendency associated with pressure work **error** has variability, the TE tendency from the $\partial\hat{E}_{phys}^{(efix)}$ has variability; $\partial\hat{E}_{phys}^{(efix)} \approx 0.30 \pm 0.08W/m^2$. As a consistency check $-\partial\hat{E}_{dyn}^{(adiab)} - \partial\hat{E}_{phys}^{(pwork)}$ is plotted with asterisk's and they coincide (as expected) with $\partial\hat{E}_{phys}^{(efix)}$ fulfilling (22).

The right-hand plot in Figure 2 shows a breakdown of the dynamical core TE tendencies. The majority of the TE errors are due to hyperviscosity on temperature and pressure, $\partial\hat{E}_{dyn}^{(hypvis)} \approx -0.61 \pm 0.01W/m^2$. The diffusion of momentum is added back as frictional heating and is therefore not part of $\partial\hat{E}_{dyn}^{(hypvis)}$. The frictional heating is a significant term in the TE tendency budget $\partial\hat{E}_{dyn}^{(heat)} \approx 0.56 \pm 0.02W/m^2$ and exhibits some variability but with a rather small amplitude. The remaining TE error in the floating Lagrangian dynamics is inviscid dissipation and time-truncation errors $\partial\hat{E}_{dyn}^{(res)} = \partial\hat{E}_{dyn}^{(2D)} - \partial\hat{E}_{dyn}^{(hypvis)} \approx 0.007W/m^2$. The TE tendency from vertical remapping is approximately $\partial\hat{E}_{dyn}^{(remap)} \approx -0.01W/m^2$. To within $\sim 0.02W/m^2$ the dynamical core TE tendency terms can be computed from just one month average TE integrals. The TE tendencies computed in physics, excluding $\partial\hat{E}_{phys}^{(param)}$, exhibit more variability and are only accurate to $\sim 0.1W/m^2$ after a one month average.

While it is advantageous to use *state-update* physics-dynamics coupling algorithm (`ftype=1`) in terms of having no spurious TE tendency from coupling, $\partial\hat{E}^{(pdc)} = 0$, it does result in spurious gravity waves in the simulations [see, e.g., Figure 5 in *Gross et al., 2018*]. Figure 3a shows a 1 year average of $|\frac{dp_s}{dt}|$, a measure of high frequency gravity wave noise. It clearly exhibits unphysical oscillations coinciding with element boundaries. Details of the spectral-element method, its coupling to physics and associated noise issues are discussed in detail in *Herrington et al. [2018]*. The noise in the solutions is even visible in the 500hPa pressure velocity annual average (Figure 4a). This issue can be alleviated by using a shorter physics time-step so that the physics increments are smaller (not shown). Climate modelers have historically not pursued a shorter physics time-step in production configurations as climate parameterizations are computationally expensive and there is a large sensitivity to physics time-steps in the simulated climate [e.g. *Williamson and Olson, 2003; Wan et al., 2015*].

3.2 ‘dribbling’ A/B: Non-TE conservative physics-dynamics coupling (`ftype=0, 2`)

3.2.1 Element boundary noise

When switching to *dribbling* physics-dynamics coupling algorithm (`ftype=0`) in which the tendencies from physics are added throughout the dynamics (in this case twice per physics time-step) then the noise issues described in previous section disappear (Figure 3b and 4b). That said, there is a significant issue with this approach; the tracer mass budgets may not be closed. How this comes about is illustrated in Figure 5 and explained in the next paragraph.

The orange curve on Figure 5a, b, d, and e is the initial state of, e.g., cloud liquid mixing ratio as a function of location, e.g., longitude. Cloud liquid is zero outside of clouds and hence provides a good example for the purpose of this illustration. The light blue arrows show the increments (in terms of length of arrow) computed by the parameterizations based on the initial state and scaled for the partial update with *dribbling* (`ftype=0`). With *state-update* (`ftype=1`) the increments from physics are added to the dynamical core state (dotted line on 5b) before the dynamical core advances the solution in time. The parameterizations are designed to not drive the mixing ratios negative so the state-update in dynamics will not generate negatives (or overshoots). Then the dynamical core advects the distribution (solid curve on Figure 5c). With *dribbling* (`ftype=0`) the physics increments are split into equal chunks (in this illustration two; blue errors on Figure 5d). Half of the physics increments are added to the initial state (dotted line on Figure 5e) and then dynamics advects the distribution half of the total dynamical core steps (dashed line on Figure 5e). Then the other half of the physics increments are applied (in the same location as they were computed by physics). Now after the previous/first advection step the cloud liquid distribution has moved and the mixing ratio may be zero (or less than the increment prescribed by physics) where the physics forcing is applied (e.g., left side of dashed curve). Hence the physics increment is driving the mixing ratios negative in those locations. Thereafter the distribution is advected (solid curve on Figure 5f). In CAM the increments added in the dynamical core are limited so that they drive the mixing to zero (but not negative) if this problem occurs. This leads to a net source of mass compared to the mass change that the parameterizations prescribe (see Figure 6). Although the average source of mass is small each time-step it always has the same sign (i.e. it is a bias) and therefore accumulates. *Zhang et al.* [2017] estimated that this spurious source of mass is equivalent to $\sim 10\text{cm}$ sea-level rise per decade in coupled climate simulation experiments.

The majority of the noise with *state-update* (`ftype=1`) physics-dynamics coupling method comes from momentum sources/sinks and heating/cooling. A way to alleviate noise problems and, at the same time, close the tracer mass budgets (in physics-dynamics coupling) is to use *state-update* (`ftype=1`) coupling for tracers and *dribbling* (`ftype=0`) coupling for momentum and temperature (referred to as *combination*, `ftype=2`). Figure 3c shows the noise diagnostic $|\frac{dps}{dt}|$ for *combination* (`ftype=2`) coupling. Figure 3c looks very similar to Figure 3b but there is some noise near element boundaries. That said, in terms of vertical pressure velocities *combination* (`ftype=2`) and *dribbling* (`ftype=0`) climates are similar in terms of the level of noise (Figure 4b and 4c). The element noise in CAM-SE with *combination* (`ftype=2`) seen in both $|\frac{dps}{dt}|$ and 500hPa pressure velocity can be ‘removed’ by using CAM-SE-CSLAM (Figure 3d) which uses a quasi equal-area physics grid and CSLAM [Conservative Semi-LAgrangian Multi-tracer; *Lauritzen et al.*, 2010] consistently coupled to the SE method [*Lauritzen et al.*, 2017]. The noise patterns in vertical velocity off the western coast of South America are present in all CAM-SE simulations (and hence not related to physics-dynamics coupling algorithm) are also ‘removed’ by using CAM-SE-CSLAM [*Herrington et al.*, 2018].

3.2.2 Spurious TE tendencies from physics-dynamics coupling

When using the same TE formula in the dynamical core and physics the spurious TE tendency from physics-dynamics coupling can be assessed. Since the pressure fields evolve during *dribbling* of physics forcing, the TE increments from the forcing change. For *dribbling* (`ftype=0`) and *combination* (`ftype=2`) this tendency is $\partial \widehat{E}^{(pdc)} = -0.05\text{W/m}^2$ and thus rather small compared to the viscosity TE dissipation rates. Since $\partial \widehat{E}^{(pdc)}$ are the same (to the second digit) for *dribbling* (`ftype=0`) and *combination* (`ftype=2`) it is the momentum and temperature *dribbling* errors that dominate $\partial \widehat{E}^{(pdc)}$.

524 3.3 *vert limiter*: Limiters on vertical remapping of momentum

525 CAM-SE uses a floating Lagrangian vertical coordinate [Starr, 1945; Lin, 2004]
 526 which requires the remapping of the atmospheric state from floating levels back to refer-
 527 ence levels to maintain computational stability and to provide state data consistent with
 528 the physics formulation. The mapping algorithm is based on the mass conservative PPM
 529 (Piecewise Parabolic Method) with options for shape-preserving limiters. In CAM-SE mo-
 530 mentum components and internal energy are used as the variables mapped in the vertical
 531 [Lauritzen *et al.*, 2018] and, contrary to earlier versions of CAM-SE, there is no limiter
 532 on the remapping of wind components. If the shape-preserving limiter is used for mo-
 533 mentum mapping then the TE dissipation increases by over an order of magnitude from
 534 $\sim 0.01W/m^2$ to $\sim 0.2W/m^2$ (Table 1).

535 3.4 *smooth topo*: Smoother topography

536 Topography for CAM is generated using a new version of the software/algorith described in Lauritzen *et al.* [2015] that is available at <https://github.com/NCAR/Topo>.
 537 The updates to the software includes smoothing algorithms and the computation of sub-
 538 grid-scale orientation of topography.

539 The default topography in CAM-SE uses the same amount of topography smoothing as CAM-FV (distance weighted smoother applied to the raw topography on $\sim 3\text{km}$
 540 cubed-sphere grid with a smoothing radius of 180km referred to as C60). When the to-
 541 polography is smoother (in this case using C92 smoothing, i.e. smoothing radius of approx-
 542 imately 276km) the hyperviscosity operators are less active leading to reduced TE errors,
 543 i.e. $\partial\widehat{E}_{dyn}^{(hvis)}$ is reduced in half from approximately $-0.6W/m^2$ to $-0.3W/m^2$. The vertical
 544 remapping TE error, however, remains approximately the same. Since the pressure work
 545 **error** is approximately $0.3W/m^2$ it almost exactly compensates for the TE tendency from
 546 the dynamical core $\partial\widehat{E}_{dyn}^{(adiab)}$. Hence if one would only diagnose the TE tendency from
 547 the energy fixer one could mistakenly conclude that the model universally conserves TE
 548 when, in fact, there are compensating TE errors in the system. These compensating errors
 549 can only be diagnosed through a careful breakdown of the total TE tendencies.

552 3.5 *default*: TE formula discrepancy errors

553 To assess the TE errors due to the discrepancy in the energy formula used by dy-
 554 namics and physics, a simulation using *state-updating* (*ftype*=1, no ‘dribbling’ errors) and
 555 thermodynamically active condensates in the dynamical core (*qsize_condensate_loading* =
 556 5) and consistent/accurate associated heat capacities $c_p^{(\ell)}$ (namelist *1cp_moist=.true.*)
 557 has been performed. In this setup the continuous equations of motion in the dynami-
 558 cal core conserve an energy different from physics, and the energy fixer will restore the
 559 ‘physics’ version of energy. Despite the dynamical core now using a more comprehensive
 560 formula for energy, the TE dissipation terms in the dynamical core are roughly the same
 561 as in the energy consistent versions of the model. Using (25) we can assess the TE energy
 562 discrepancy errors which result in $\sim 0.59W/m^2$. Taylor [2011] found a similar result just
 563 from using the more comprehensive formula for heat capacity (based on dry air and wa-
 564 ter vapor) and not including thermodynamically active condensates. As noted before this
 565 formulation inconsistency is due to the evolutionary nature of CAM development and it is
 566 the intention to remove this inconsistency in future versions of the model.

567 The default version of CAM-SE uses this configuration but with *combination* (*ftype*=2)
 568 which has similar TE characteristics (see Table 1). That said, the physics-dynamics cou-
 569 pling error from *dribbling* momentum and temperature tendencies and the energy discrep-
 570 ancy errors can not be separated in this configuration:

$$\partial\widehat{E}^{(pdc)} + \partial\widehat{E}^{(discr)} = 0.546W/m^2, \quad (26)$$

571 using (22). With *state-updating* (*ftype*=1) (i.e. $\partial\widehat{E}^{(pdc)} = 0$) the energy discrepancy error
 572 was $0.594W/m^2$ and in the energy consistent setup (i.e. $\partial\widehat{E}^{(discr)} = 0$) but using *dribbling*
 573 (*ftype*=2) we got $\partial\widehat{E}^{(pdc)} = 0.484W/m^2$. So if the physics-dynamics coupling errors
 574 and energy discrepancy errors in the different configurations would be additive, one would
 575 have expected $\partial\widehat{E}^{(pdc)} + \partial\widehat{E}^{(discr)}$ to be over $1W/m^2$ which is clearly not the case (26).
 576 Again, it must be concluded that there are canceling errors in the system.

577 3.6 QPC6: Simplified surface

578 By running the model in aqua-planet configuration one can assess the effect of sim-
 579 plifying the surface boundary condition. In particular, without topography forcing the dy-
 580 namical core is not challenged with respect to stationary near-grid-scale forcing. The TE
 581 tendency with respect to pressure work **error** remains the same $\partial\widehat{E}_{phys}^{(pwork)}$ as the AMIP-
 582 type simulations, however, the adiabatic dynamical core TE tendency reduces to $\partial\widehat{E}_{dyn}^{(adiab)} =$
 583 $-0.14W/m^2$ (approximately a factor 4 reduction). Most of that reduction is due to viscos-
 584 ity $\partial\widehat{E}_{dyn}^{(hvis)} = -0.13W/m^2$. The frictional heating is roughly the same as AMIP $\partial\widehat{E}_{dyn}^{(fheat)} =$
 585 $0.48W/m^2$ as is the vertical remapping $\partial\widehat{E}_{dyn}^{(remap)} = -0.01W/m^2$. To evaluate the dynam-
 586 ical cores diffusion of TE it is therefore important to asses the model in a configuration
 587 with topography as the wave dynamics generated by topography leads to more active dif-
 588 fusion operators.

589 3.7 FHS94: Simplified physics (no moisture)

590 Simplifying the setup even further by replacing the parameterizations with relax-
 591 ation towards a zonally symmetric temperature profile and simple boundary layer friction
 592 (Held-Suarez forcing) as well as excluding moisture, the TE errors in the dynamical core
 593 decreases even further to $\sim 0.002W/m^2$ since there is no small scale forcing. Small scales
 594 are only created by the nonlinear dynamics and the physics works to damp them. Hyper-
 595 viscosity is less active leading to significant reductions compared to aqua-planet and ‘real-
 596 world’ simulation results. The TE diffusion in vertical remapping reduces by an order of
 597 magnitude compared to the aqua-planet simulations ($\sim 0.0005W/m^2$). This further em-
 598 phasizes that TE diffusion assessment in a simplified setup is not necessarily telling for
 599 the dynamical cores performance with moist physics and topography that challenge the
 600 dynamical core in terms of strong grid-scale forcing.

601 3.8 FV: Changing dynamical core to Finite-Volume (FV)

602 As a comparison the TE error characteristics of the CAM-FV dynamical core are
 603 assessed. Although the TE diagnostics have not been implemented in the CAM-FV dy-
 604 namical core, the TE diagnostics in CAM physics are independent of dynamical core
 605 and can therefore be activated with CAM-FV. The CAM-FV dynamical core uses *state-*
 606 *update* physics-dynamics coupling (*ftype*=1) ($\partial\widehat{E}^{(pdc)} = 0$) and the same TE definition
 607 as CAM physics ($\partial\widehat{E}^{(discr)} = 0$). Hence (23) can be used to compute the TE errors of
 608 the CAM-FV dynamical core, $\partial\widehat{E}_{dyn}^{(adiab)} \approx -1W/m^2$. As we do not have the break-down
 609 of $\partial\widehat{E}_{dyn}^{(adiab)}$ it can not be determined how much of the TE errors are due to the vertical
 610 remapping. Furthermore, CAM-FV contains intrinsic dissipation operators (limiters in the
 611 flux operators) making it difficult to assess TE sources/sinks due to dissipation. Note that
 612 the pressure work **error** even with a change of dynamical core remains approximately the
 613 same as the CAM-SE configurations.

614 3.9 CSLAM: Quasi equal-area physics grid

615 This configuration was discussed in the context of element noise in section 3.2.1.
 616 By averaging the dynamics state of an equal-partitioning (in central angle cubed-sphere

coordinates) of the elements, the element-boundary noise found in CAM-SE can be removed. Lauritzen *et al.* [2018] argue that this way of computing the state for the physics is more consistent with physics in terms of providing a cell-averaged state instead of irregularly spaced point (quadrature) values. In order to achieve a closed mass-budget, this configuration uses CSLAM for tracer transport rather than SE transport. That said, the physics columns no longer coincide with the quadrature grid and there are TE errors associated with mapping state and tendencies between the two grids.

In this configuration the energy diagnostics computed in the dynamical core are computed on the quadrature grid and the energy diagnostics computed in physics are on the physics grid. If the TE consistent configuration is used (`ftype=1, qsize_condensate_loading=1, lcp_moist=.false.`) then the physics-dynamical coupling errors, $\widehat{E}^{(pdc)}$ computed with (20), are entirely due to mapping state from quadrature grid to physics grid and mapping tendencies back the quadrature grid from the physics grid. The results is $\widehat{E}^{(pdc)} = -0.07W/m^2$ which is a rather small error compared to other terms in the TE budget.

Due to similar noise problems with CAM-SE-CSLAM when using `ftype=1` that were observed in CAM-SE (Figure 3 and 4), the default version of CAM-SE-CSLAM uses `ftype=2`. Again physics-dynamics coupling errors and TE discrepancy errors can not be separated; $\partial\widehat{E}^{(pdc)} + \partial\widehat{E}^{(discr)} = 0.557W/m^2$.

4 Conclusions

A detailed total energy (TE) error analysis of the Community Atmosphere Model (CAM) using version 6 physics (included in the CESM2.1 release) running at approximately 1° horizontal resolution has been presented. In the global climate model there can be many spurious contributions to the TE budget. These errors can be divided into four categories: physical parameterizations, adiabatic dynamical core, the coupling between physics and dynamics, and TE definition discrepancies between dynamics and physics. The latter is not by design but through the evolutionary nature of model development. By capturing the atmospheric state at various locations in the model algorithm, a detailed budget of TE errors can be constructed. The net spurious TE energy errors are compensated with a global energy fixer (providing a global uniform temperature increment) every physics time-step.

In CAM physics the parameterizations have, by design, a closed energy budget (change in TE is balanced by fluxes in/out the top and bottom of physics columns) if it is assumed that pressure is not modified. However, the pressure changes due to fluxes of mass (e.g., water vapor) in/out of the column which changes energy (referred to as pressure work **error**). The pressure work **error** with the full moist physics configuration is very stable across different configurations at $\sim 0.3W/m^2$. The TE errors in the spectral element (SE) dynamical core varies across configurations. Aspects that influence TE is the presence of topography, the amount of topography smoothing and moist physics. By smoothing topography more the TE error is cut in half from $\sim -0.6W/m^2$ to $\sim -0.3W/m^2$, and reduces by a factor of five ($\sim -0.1W/m^2$) if no topography is present at all (aqua-planet configuration). Moist physics forcing also contributes significantly to the TE budget. For example, in the dry Held-Suarez setup TE dissipation of the SE dynamical core reduces to $-0.03W/m^2$. Topography and moist physics force the dynamical core at the grid scale and hence the viscosity operators are more active. Consistent with this statement is that the changes in TE discussed so far are almost entirely due to the viscosity operator TE dissipation. For CAM-SE the spurious TE dissipation in the adiabatic dynamical core is $\sim -0.6W/m^2$ in ‘real-world’ configurations. For comparison, CAM-FV’s spurious TE change due to the adiabatic dynamical core is $\sim -1W/m^2$.

By further breaking down the TE dissipation in the SE dynamical core it is observed the vertical remapping accounts for only $\sim -0.01W/m^2$. That said, if the shape-

preserving limiters in the vertical remapping are invoked the TE dissipation increases 20-fold to $\sim -0.2W/m^2$. In CAM-SE the kinetic energy dissipation is added as heating in the thermodynamic equation (also referred to as frictional heating). The frictional heating remains very stable across configurations that include moisture ($\sim 0.5W/m^2$) and reduces drastically for dry atmosphere setups (factor 4 reduction to ($\sim 0.12W/m^2$)). Hence this term is an important term in the TE budget. The TE budget for the dynamical core is dominated by TE change due to hyperviscosity; TE errors due to time-truncation and frictionless equations of motion are negligible. Errors associated with physics-dynamics coupling (if applicable) are approximately $0.5W/m^2$. Due to the evolutionary nature of model development the SE dynamical core's continuous equation of motion conserve a more comprehensive TE compared to the physical parameterizations. This TE discrepancy leads to an approximately $0.5W/m^2$ total energy source. Running physics on a different grid than the dynamical introduces TE mapping errors such as in CAM-SE-CSLAM (Conservative Semi-Lagrangian Multi-tracer transport scheme). These errors are, however, rather small $-0.07W/m^2$.

A purpose of this paper is to better understand the energy characteristics of CAM and to encourage modeling groups to perform similar analysis to better understand the total energy flow in the atmospheric component of Earth system models. As has been demonstrated in this paper there can easily be compensating errors in the system which can not be identified without a detailed TE analysis.

Acknowledgments

The National Center for Atmospheric Research is sponsored by the National Science Foundation. Computing resources (doi:10.5065/D6RX99HX) were provided by the Climate Simulation Laboratory at NCAR's Computational and Information Systems Laboratory, sponsored by the National Science Foundation and other agencies. The data used to perform the energy analysis can be found at <https://github.com/PeterHjortLauritzen/2018-JAMES-energy>.

References

- Boville, B. (2000), chap. Toward a complete model of the climate system in Numerical Modeling of the Global Atmosphere in the Climate System, pp. 419–442, Springer Netherlands.
- Computational and Information Systems Laboratory (2017), Cheyenne: HPE/SGI ICE XA System (Climate Simulation Laboratory), Boulder, CO: National Center for Atmospheric Research, doi:10.5065/D6RX99HX.
- Eldred, C., and D. Randall (2017), Total energy and potential enstrophy conserving schemes for the shallow water equations using hamiltonian methods – part 1: Derivation and properties, *Geosci. Model Dev.*, 10(2), 791–810, doi:10.5194/gmd-10-791-2017.
- Gross, M., H. Wan, P. J. Rasch, P. M. Caldwell, D. L. Williamson, D. Klocke, C. Jablonowski, D. R. Thatcher, N. Wood, M. Cullen, B. Beare, M. Willett, F. Lemarié, E. Blayo, S. Malardel, P. Termonia, A. Gassmann, P. H. Lauritzen, H. Johansen, C. M. Zarzycki, K. Sakaguchi, and R. Leung (2018), Physics-dynamics coupling in weather, climate and earth system models: Challenges and recent progress, *Mon. Wea. Rev.*, 146, 3505–3544, doi:10.1175/MWR-D-17-0345.1.
- Held, I. M., and M. J. Suarez (1994), A proposal for the intercomparison of the dynamical cores of atmospheric general circulation models, *Bull. Amer. Meteor. Soc.*, 75, 1825–1830.
- Herrington, A. R., P. H. Lauritzen, M. A. Taylor, S. Goldhaber, B. E. Eaton, K. A. Reed, and P. A. Ullrich (2018), Physics-dynamics coupling with element-based high-order Galerkin methods: quasi equal-area physics grid, *Mon. Wea. Rev.*

- 719 Jablonowski, C., and D. L. Williamson (2011), chap. The Pros and Cons of Diffusion,
 720 Filters and Fixers in Atmospheric General Circulation Models, pp. 381–493, Springer
 721 Berlin Heidelberg, Berlin, Heidelberg, doi:10.1007/978-3-642-11640-7_13.
- 722 Kasahara, A. (1974), Various vertical coordinate systems used for numerical weather pre-
 723 diction, *Mon. Wea. Rev.*, 102(7), 509–522.
- 724 Lauritzen, P. H., R. D. Nair, and P. A. Ullrich (2010), A conservative semi-Lagrangian
 725 multi-tracer transport scheme (CSLAM) on the cubed-sphere grid, *J. Comput. Phys.*,
 726 229, 1401–1424, doi:10.1016/j.jcp.2009.10.036.
- 727 Lauritzen, P. H., J. T. Bacmeister, T. Dubos, S. Lebonnois, and M. A. Taylor (2014),
 728 Held-Suarez simulations with the Community Atmosphere Model Spectral Element
 729 (CAM-SE) dynamical core: A global axial angular momentum analysis using Eule-
 730 rian and floating Lagrangian vertical coordinates, *J. Adv. Model. Earth Syst.*, 6, doi:
 731 10.1002/2013MS000268.
- 732 Lauritzen, P. H., J. T. Bacmeister, P. F. Callaghan, and M. A. Taylor (2015), NCAR_Topo
 733 (v1.0): NCAR global model topography generation software for unstructured grids,
 734 *Geosci. Model Dev.*, 8(12), 3975–3986, doi:10.5194/gmd-8-3975-2015.
- 735 Lauritzen, P. H., M. A. Taylor, J. Overfelt, P. A. Ullrich, R. D. Nair, S. Goldhaber, and
 736 R. Kelly (2017), CAM-SE-CSLAM: Consistent coupling of a conservative semi-
 737 lagrangian finite-volume method with spectral element dynamics, *Mon. Wea. Rev.*,
 738 145(3), 833–855, doi:10.1175/MWR-D-16-0258.1.
- 739 Lauritzen, P. H., R. Nair, A. Herrington, P. Callaghan, S. Goldhaber, J. Dennis, J. T.
 740 Bacmeister, B. Eaton, C. Zarzycki, M. A. Taylor, A. Gettelman, R. Neale, B. Dobbins,
 741 K. Reed, and T. Dubos (2018), NCAR release of CAM-SE in CESM2.0: A reformu-
 742 lation of the spectral-element dynamical core in dry-mass vertical coordinates with
 743 comprehensive treatment of condensates and energy, *J. Adv. Model. Earth Syst.*, doi:
 744 10.1029/2017MS001257.
- 745 Lin, S.-J. (2004), A 'vertically Lagrangian' finite-volume dynamical core for global mod-
 746 els, *Mon. Wea. Rev.*, 132, 2293–2307.
- 747 McRae, A. T. T., and C. J. Cotter (2013), Energy- and enstrophy-conserving schemes for
 748 the shallow-water equations, based on mimetic finite elements, *Quart. J. Roy. Meteor.
 749 Soc.*, 140(684), 2223–2234, doi:10.1002/qj.2291.
- 750 Medeiros, B., D. L. Williamson, and J. G. Olson (2016), Reference aquaplanet climate in
 751 the community atmosphere model, version 5, *J. Adv. Model. Earth Syst.*, 8(1), 406–424,
 752 doi:10.1002/2015MS000593.
- 753 Neale, R. B., and B. J. Hoskins (2000), A standard test for AGCMs including their phys-
 754 ical parametrizations: I: the proposal, *Atmos. Sci. Lett.*, 1(2), 101–107, doi:10.1006/asle.
 755 2000.0022.
- 756 Neale, R. B., C.-C. Chen, A. Gettelman, P. H. Lauritzen, S. Park, D. L. Williamson, A. J.
 757 Conley, R. Garcia, D. Kinnison, J.-F. Lamarque, D. Marsh, M. Mills, A. K. Smith,
 758 S. Tilmes, F. Vitt, P. Cameron-Smith, W. D. Collins, M. J. Iacono, R. C. Easter, S. J.
 759 Ghan, X. Liu, P. J. Rasch, and M. A. Taylor (2012), Description of the NCAR Commu-
 760 nity Atmosphere Model (CAM 5.0), *NCAR Technical Note NCAR/TN-486+STR*, National
 761 Center of Atmospheric Research.
- 762 Skamarock, W. C., J. B. Klemp, M. G. Duda, L. Fowler, S.-H. Park, and T. D. Ringler
 763 (2012), A multi-scale nonhydrostatic atmospheric model using centroidal Voronoi tes-
 764 selations and C-grid staggering, *Mon. Wea. Rev.*, 240, 3090–3105, doi:doi:10.1175/
 765 MWR-D-11-00215.1.
- 766 Starr, V. P. (1945), A quasi-Lagrangian system of hydrodynamical equations., *J. Atmos.
 767 Sci.*, 2, 227–237.
- 768 Taylor, M. A. (2011), Conservation of mass and energy for the moist atmospheric prim-
 769 itive equations on unstructured grids, in: P.H. Lauritzen, R.D. Nair, C. Jablonowski,
 770 M. Taylor (Eds.), Numerical techniques for global atmospheric models, *Lecture Notes
 771 in Computational Science and Engineering*, Springer, 2010, *in press.*, 80, 357–380, doi:
 772 10.1007/978-3-642-11640-7_12.

- 773 Thuburn, J. (2008), Some conservation issues for the dynamical cores of NWP and cli-
774 mate models, *J. Comput. Phys.*, 227, 3715–3730.
- 775 Trenberth, K. E., and J. T. Fasullo (2018), Applications of an updated atmospheric ener-
776 getics formulation, *J. Climate*, 31(16), 6263–6279, doi:10.1175/JCLI-D-17-0838.1.
- 777 Wan, H., P. J. Rasch, M. A. Taylor, and C. Jablonowski (2015), Short-term time step con-
778 vergence in a climate model, *J. Adv. Model. Earth Syst.*, 7(1), 215–225, doi:10.1002/
779 2014MS000368.
- 780 Williamson, D. L. (2002), Time-split versus process-split coupling of parameterizations
781 and dynamical core, *Mon. Wea. Rev.*, 130, 2024–2041.
- 782 Williamson, D. L., and J. G. Olson (2003), Dependence of aqua-planet simulations on
783 time step, *Q. J. R. Meteorol. Soc.*, 129(591), 2049–2064.
- 784 Williamson, D. L., J. G. Olson, C. Hannay, T. Tonietto, M. Taylor, and V. Yudin (2015),
785 Energy considerations in the community atmosphere model (cam), *J. Adv. Model. Earth
786 Syst.*, 7(3), 1178–1188, doi:10.1002/2015MS000448.
- 787 Zhang, K., P. J. Rasch, M. A. Taylor, H. Wan, L.-Y. R. Leung, P.-L. Ma, J.-C. Golaz,
788 J. Wolfe, W. Lin, B. Singh, S. Burrows, J.-H. Yoon, H. Wang, Y. Qian, Q. Tang,
789 P. Caldwell, and S. Xie (2017), Impact of numerical choices on water conservation in
790 the e3sm atmosphere model version 1 (eam v1), *Geoscientific Model Development Dis-
cussions*, 2017, 1–26, doi:10.5194/gmd-2017-293.

```

do nt=1,ntotal

PARAMETERIZATIONS:
Last dynamics state received from dynamics
output 'pBF'
efix Energy fixer
output 'pBP'
phys param Physics updates the state and state saved for energy fixer
output 'pAP'
pwork Pressure work (dry mass correction)
output 'pAM'
Physics tendency (forcing) passed to dynamics

DYNAMICAL CORE
output 'dED'
do ns=1,nsplit
output 'dAF'

phys
START PHYSICS-DYNAMICS COUPLING
Update dynamics state with (1/nsplit) of physics tendency (ftype=2)
if (ns=1) Update dynamics state with entire physics tendency (ftype=1)
DONE PHYSICS-DYNAMICS COUPLING

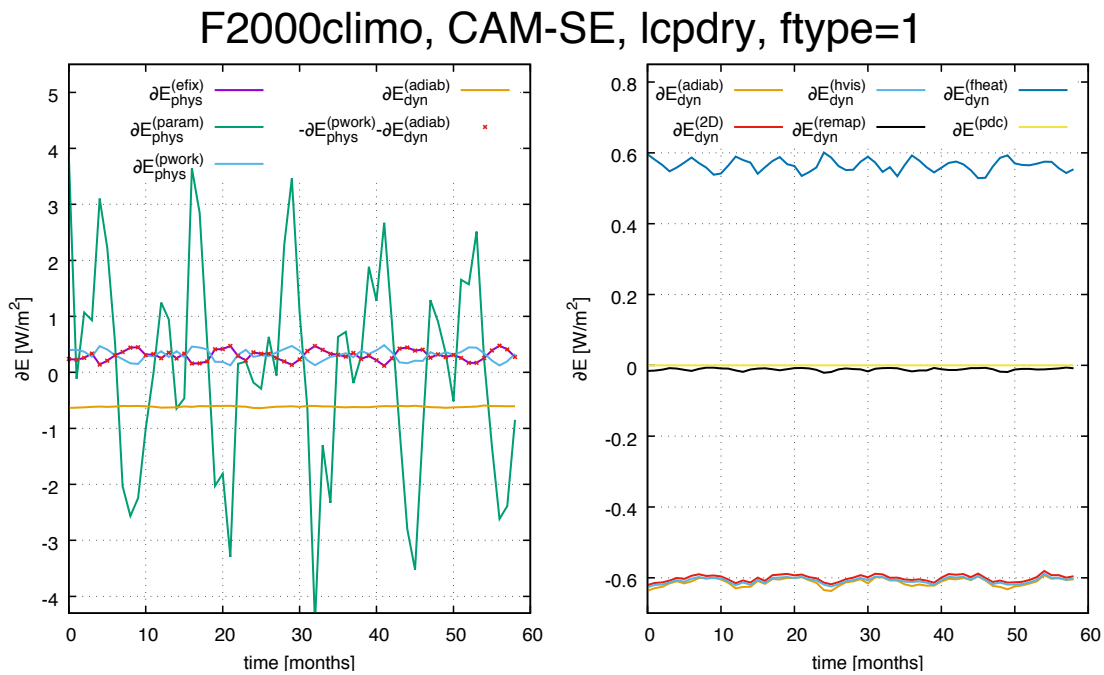
output 'dB'D'

adiab
2D
hvis
do nr=1,rsplit
Advance the adiabatic frictionless equations of motion
in floating Lagrangian layer
do ns=1,hypervis_subcycle
output 'dBH'
Apply hyperviscosity operators
output 'dCH'
fheat Add frictional heating to temperature
output 'dAH'
end do (ns=1,hypervis_subcycle)
end do (nr=1,rsplit)
output 'dAD'
remap
Vertical remapping from floating Lagrangian levels to Eulerian levels
output 'dAR'
end do (ns=1,nsplit)
Dynamics state saved for next model time step and passed to physics
output 'dB'F'

end do (nt=1,ntotal)

```

259 **Figure 1.** Pseudo-code for CAM-SE showing the order in which relevant physics updates are performed as
260 well as dynamical core steps and associated loops. In green font locations where the state is captured and out-
261 put is shown together with its 3 character identifier. The outer most loop (1, *ntotal*) advances the entire model
262 Δt_{phys} seconds (in this case 1800s). The dynamical core loops are as follows: the outer loop is the vertical
263 remapping loop (1, *nsplit*) with associated time-step $\Delta t_{phys}/nsplit$. For stability the temporal advance-
264 ment of the equations of motion in the Lagrangian layer needs to be sub-cycled *rsplit* times. Within the
265 *rsplit*-loop the hyperviscosity time-stepping is sub-cycled *hypervis_subcycle* times (again for stability).
For more details on the time-stepping in CAM-SE see Lauritzen *et al.* [2018].



408 **Figure 2.** Monthly averaged TE tendencies as a function of time for various aspects of the TE consistent
 409 configuration of CAM-SE run in AMIP-type configuration with perpetual year 2000 SSTs. Left Figure shows
 410 $\partial \widehat{E}$ TE tendencies in physics and, for comparison, TE tendency for the adiabatic dynamical core. The right
 411 plot shows the break-down of $\partial \widehat{E}$ for the dynamical core. These plots show that the energy tendency from the
 412 dynamical core is quite constant (to within $\sim 0.02 W/m^2$ or less) so only one month simulations is adequate to
 413 assess energy diagnostics for the dynamical core. For more details see Section 3.1.

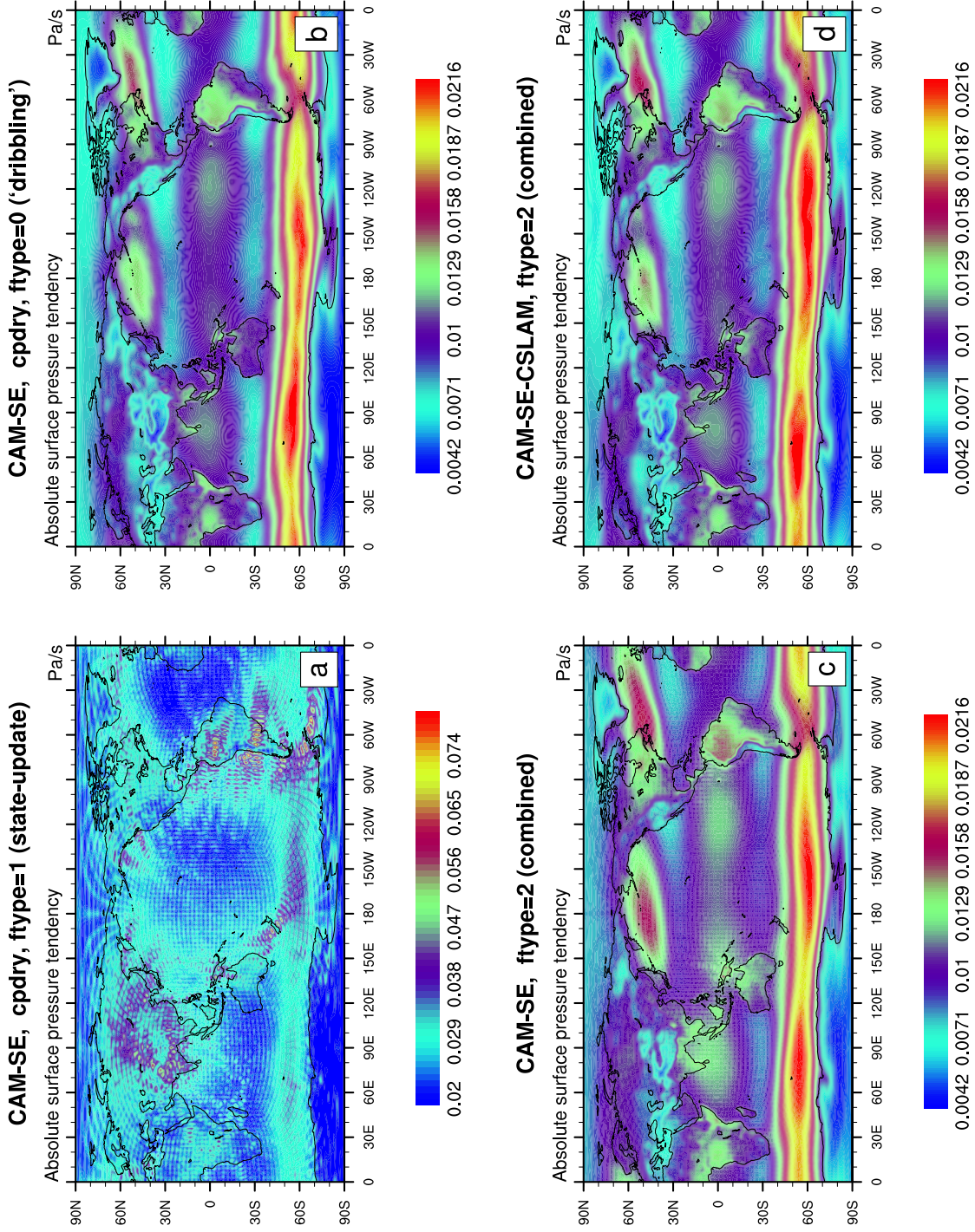


Figure 3. One year average of the absolute surface pressure tendency for (a) the TE consistent configuration, (b) ‘dribbling’ physics-dynamics coupling, (c) ftype=2 physics-dynamics coupling and (d) CSLAM version of CAM-SE, respectively. (a) has a closed physics-dynamics coupling budget but spurious noise, (b) has no spurious noise but the mass-budget in physics-dynamics coupling is not closed (see Figure 6), (c) has a closed mass budget in physics-dynamics coupling but some spurious noise at element boundaries which is eliminated when using CAM-SE-CSLAM (d). Note, the smallest value in panel (a) is the largest in panels (b), (c) and (d).

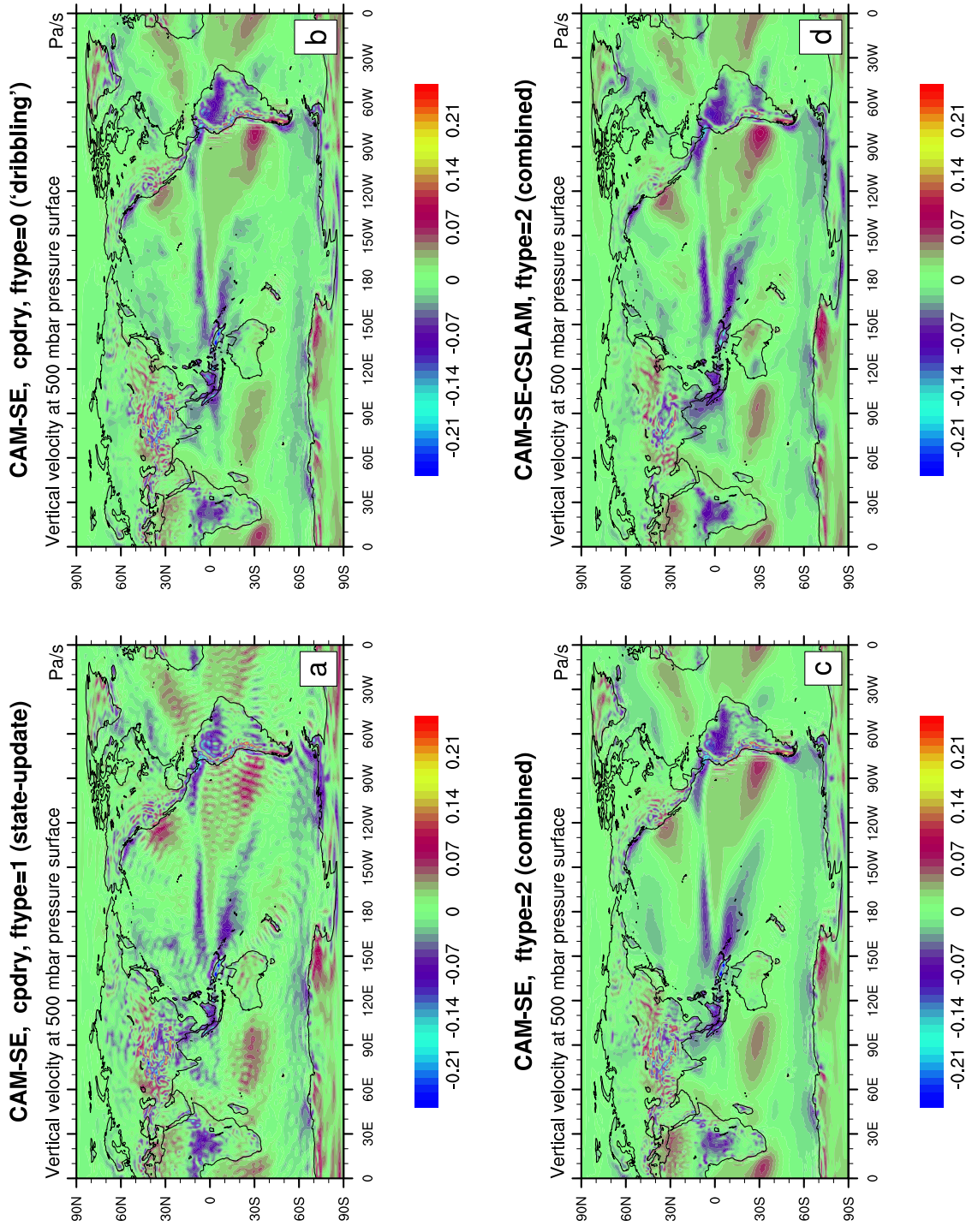


Figure 4. Same as Figure 3 but for 500hPa vertical pressure velocity. Note the ringing patterns off the West coast of South America and around the Himalayas in CAM-SE (a-c) that are eliminated with CAM-SE-CSLAM (d) that makes use of a quasi equal-area physics grid.

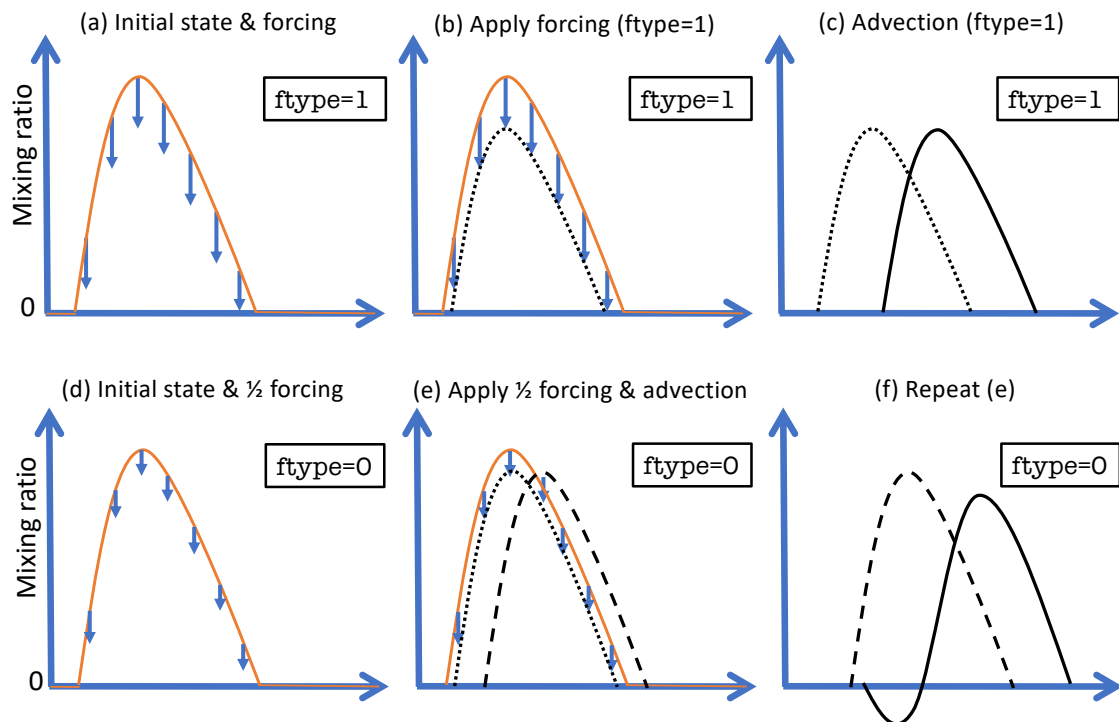


Figure 5. A schematic of state-update ($\text{ftype}=1$; row 1) and ‘dribbling’ ($\text{ftype}=0$; row 2) physics-dynamics coupling algorithms. See Section 3.2 for details.

F2000climo, CAM-SE, cpdry, ftype=0 ('dribbling')

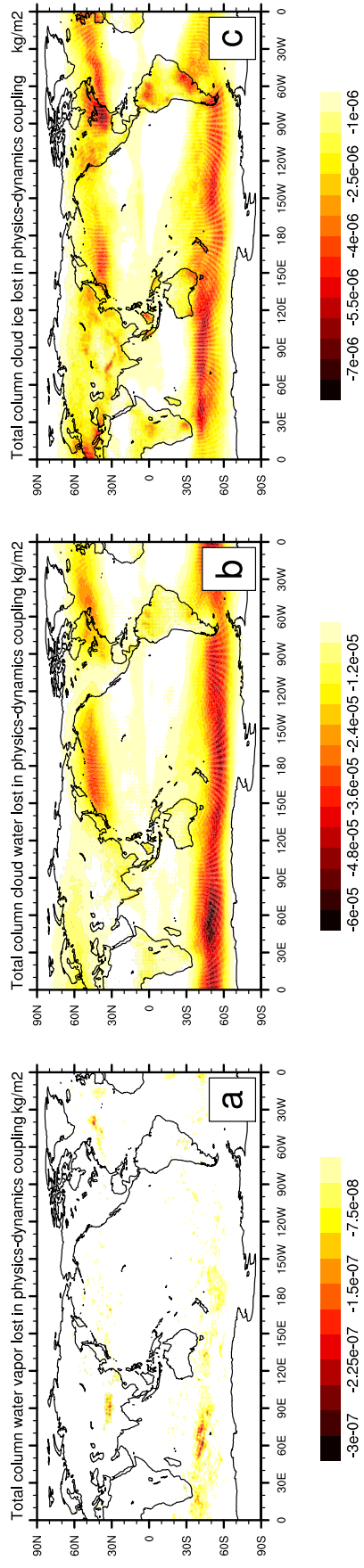


Figure 6. One year average of mass [kg/m^2] 'clipped' in physics-dynamics coupling (so that state is not driven negative) when using `ftype=0` ('dribbling') physics-dynamics coupling for (a) water vapor, (b) cloud liquid and (c) cloud ice, respectively. Interestingly the element boundaries systematically show in the plots which is likely related to the anisotropy of the quadrature grid [Herrington *et al.*, 2018].